Effect of the Addition of Inert or TEMPO-Capped Prepolymer on Polymerization Rate and Molecular Weight Development in the Nitroxide-Mediated Radical Polymerization of Styrene

Martha Roa-Luna,[1]* Afsaneh Nabifar,[2] Neil T. McManus,[2] Eduardo Vivaldo-Lima,[1] Liliane M. F. Lona,[3] Alexander Penlidis[2]

[1]*Facultad de Química, Departamento de Ingeniería Química, Universidad Nacional Autónoma de México, México D. F. 04510, México*
[2]*Institute for Polymer Research (IPR), Department of Chemical Engineering, University of Waterloo, Waterloo, Ontario N2L 3G1, Canada*
[3]*Universidade Estadual de Campinas, Faculdade de Engenharia Química, Departamento de Processos Químicos, CP 6066 CEP: 13083-970, Campinas, Sao Paulo, Brazil*

Received 7 August 2007; accepted 24 March 2008
DOI 10.1002/app.28507
Published online 4 June 2008 in Wiley InterScience (www.interscience.wiley.com).

ABSTRACT: The importance of diffusion-controlled (DC) effects on controlled radical polymerization (CRP) processes has been rather controversial and usually considered only if there is some mismatch between experimental data and model predictions of polymerization rate and molecular weight averages. Results from an experimental study designed to create conditions in which DC effects may be present from the outset for the bimolecular nitroxide-mediated radical polymerization (NMRP) of styrene in the presence of 2,2,6,6-tetramethyl-1-piperidinyloxy (TEMPO) and dibenzoyl peroxide (BPO), are presented herein. The experiments consisted of adding size exclusion chromatography (SEC) polystyrene (PS) standards or nitroxyl-capped PS (of different molecular weights, in several proportions), to a conventional recipe of bimolecular NMRP of styrene, and studying the effect of their presence on polymerization rate and molecular weight development. A previously developed kinetic model for NMRP of styrene was modified to take into account the presence of prepolymer as an inert ''solvent,'' or as a monomolecular ''controller'' of high molecular weight. The effects of DC reactions (propagation, termination, activation, and deactivation of polymer radicals) were modeled using conventional free-volume theory. Reasonably, good agreement between experimental data and model predictions with either modeling approach was obtained. It was concluded that DC effects are weak in the NMRP of styrene, even in the presence of prepolymer. J Appl Polym Sci 109: 3665–3678, 2008

Key words: living polymerization; radical polymerization; kinetics of polymerization; modeling; polystyrene

INTRODUCTION

Nitroxide-mediated radical polymerization (NMRP) is a very important synthetic route for the production of well-defined block and graft copolymers, gradient and periodic copolymers, stars, combs, polymer networks, end-functional polymers, and many other materials with controlled microstructure.[1] Polymeric materials synthesized by NMRP can be used as coatings, adhesives, surfactants, dispersants, lubricants, gels, additives, and thermoplastic elastomers as well as materials for biomedical applications.[1] Stabilizers synthesized by NMRP on a commercial scale have been produced.[2–4] The chemistry[5] and other kinetic/mechanistic aspects[6–14] of NMRP are nowadays relatively well understood. Detailed kinetic models that describe polymerization rate and molecular weight development of NMRP are available in the open literature.[15–17]

The effects of diffusion-controlled (DC) reactions on controlled radical polymerization (CRP) processes have not been studied and understood as systematically as in standard free-radical polymerization. Some authors have considered these effects negligible for NMRP due to the low molecular weights typical of CRP, others only consider DC-termination in

**Present address:* Facultad de Ciencias Químicas, Universidad Veracruzana, Av. Universidad Veracruzana Km. 7.5, Coatzacoalcos, Veracruz, México.
Correspondence to: E. Vivaldo-Lima (vivaldo@servidor.unam.mx).
Contract grant sponsors: CONACYT, Mexico; contract grant number: CIAM U40259-Y.
Contract grant sponsors: NSERC, Canada, and CNPQ, Brazil, through Inter American Materials Collaboration (IAMC or CIAM), Department of Chemical Engineering of the University of Waterloo, DGEP-UNAM, DGAPA-UNAM (PASPA).

TABLE I
Experimental Conditions

Run No.	T (°C)	[BPO] (mol/L)	[TEMPO]/[BPO]	Mol. Wt. of prepolymer (g/mol)	Prepolymer identifier	Wt% Prepolymer (effective molar concentration, mole per liter)
1	120	0.0192	1.073	17,400 (M_n); PDI = 1.22	PPS II	44.94 (0.016)
2	120	0.03321	0.9945	5,000 (M_n); PDI < 1.1	PPS I	5.15 (0.0086)
3	120	0.03048	1.119	900,000 (M_{peak}); PDI < 1.1	PPS V	5.17 (4.78×10^{-5})
4	130	0.036	1.1	738,000 (M_n); PDI = 1.04	PPS IV	4.48 (4.89×10^{-5})
5	130	0.036	1.1	1,210,000 (M_n); PDI = 1.02	PPS VI	4.48 (2.986×10^{-5})
6	130	0.036	1.1	182,000 (M_n); PDI = 1.03	PPS III	4.48 (1.922×10^{-4})

a semiempirical fashion,[15,18,19] and others consider that the reactions of propagation, activation, and deactivation of polymer radicals may also become DC.[20,21] Chevalier et al.[22] carried out an experimental study on the effect of dilution on the termination kinetic rate constant, k_t, in the NMRP of styrene, using *N-tert*-butyl-*n*-(1-diethylphosphono-2,2-dimethylpropyl)-*n*-oxyl (SG1), at 120°C, and found that k_t was independent of viscosity build-up induced by monomer conversion, but there seemed to be a dependence of the value of k_t on the initial dilution of the system. However, the variations observed would have no influence on calculations of polymerization rate and molecular weight development in free-radical polymerization processes.

In our group, we have carried out a systematic study on the effects of DC reactions on the polymerization kinetics and molecular weight development in NMRP of styrene using 2,2,6,6-tetramethyl-1-piperidinyloxy (TEMPO) and dibenzoyl peroxide (BPO). The first stage of this study was to expand and validate[23] a previously derived[16] kinetic model, using experimental data from our laboratories, now reported in the literature.[24] This was followed by modifying the model with the incorporation of DC effects.[21] Because DC effects seemed to be weak in NMRP, physical means to promote them were also attempted. The first approach was to add small amounts of crosslinker (divinylbenzene, DVB) with the idea of promoting higher molecular weights and thus, higher viscosities, from early on in the reaction.[25] The second approach, reported herein, consisted of carrying out NMRP experiments in the presence of prepolymer, also with the idea of promoting high viscosities from early on in the reaction, but avoiding the formation of a polymer network. Inert [size exclusion chromatography (SEC) standards] and dormant (TEMPO-capped polymer produced in our laboratory) prepolymers of different molecular weights, in different proportions and two different temperatures, were added at time zero. The analysis was done with the help of simulations considering DC effects and the presence of prepolymer (either as inert ''solvent,'' or as monomolecular controller of high molecular weight), carried out with the Predici® commercial software.

EXPERIMENTAL

Reagents and purification methods

Styrene (Aldrich Chemical, Toluca, Mexico, 99% S4972-4L), was washed, dried, and distilled using standard purification methods.[26] TEMPO (Aldrich Chemical, 99%, sublimed, 42,636-9-5G, 2564-83-2) was used as received. However, its purity was checked by measuring the effective concentration of aminoxyl (nitroxyl) free radicals in toluene solution in a Bruker (Mexico City, Mexico) ELEXSYS 500 electron spin resonance (ESR) spectrometer. BPO from AKZO (Edo. de Mexico, Mexico) (PXIW75, 75% BPO, and 25% water) was recrystallized from methanol thrice.[24]

TEMPO-capped prepolymer (with a small proportion of inert polystyrene (PS) caused by bimolecular termination during the production of the TEMPO-capped prepolymer) was obtained from bimolecular NMRP experiments.[24] Two values of number–average molecular weight, M_n, were used as shown in Table I (runs 1 and 2). The inert prepolymer, with values of molecular weight also shown in Table I (runs 3–6), consisted of PS SEC standards, supplied by Polymer Standards Service (Waters Mexico, Mexico City, Mexico).

The other chemicals, methanol (Baker, 99.9%), dichloromethane (Baker), sodium hydroxide (98%, Aldrich), hydroquinone (Aldrich HI790-2, 99%), and tetrahydrofuran (THF) (HPLC grade, Caledon Laboratories, Zapopan, Jalisco, Mexico, or Baker), were used without further purification.

Polymerization method

Solutions were prepared with the appropriate amounts of TEMPO, BPO, styrene, and prepolymer according to the recipes described in Table I. Aliquots of the solution were then transferred into ampoules (5-mm outer diameter). The contents of the ampoules were degassed by three successive freeze-thaw cycles under vacuum (0.03 mbar). The ampoules were torch sealed under vacuum and then placed in liquid nitrogen until used. The polymerizations were carried out in a Neslab circulator bath, containing silicone oil, with temperature control at the predetermined temperature (120°C or 130°C ±

TABLE II
Kinetic Parameters Used in the Simulations

Parameter	Value or Function	Reference
k_{di} (s^{-1})	$1.7\times10^{15}\exp\left(-\frac{3000}{RT}\right)$	15
f_0	0.55	15
k_{dim} (L mol^{-1} s^{-1})	$188.97\exp\left(-\frac{16185.1}{RT}\right)$	23
k_{ia} (L mol^{-1} s^{-1})	$6.359\times10^{12}\exp\left(-\frac{36598.55}{RT}\right)$	23
k_{p0} (L mol^{-1} s^{-1})	$4.266\times10^{7}\exp\left(-\frac{7769.17}{RT}\right)$	15
k_{t0} (L mol^{-1} s^{-1})	$2.002\times10^{10}\exp\left(-\frac{3081.84}{RT}\right)$	15
$k_{td}/(k_{tc0} + k_{td0})$	0.0	23
k_{fm} (L mol^{-1} s^{-1})	0.0	Neglected
k_{fd} (L mol^{-1} s^{-1})	0.0	Neglected
k_d (L mol^{-1} s^{-1})	$5.03\times10^{9}\exp\left(-\frac{3722}{RT}\right)$	15
k_a (s^{-1})	$2.0\times10^{13}\exp\left(-\frac{29683}{RT}\right)$	15
k_{decomp} (s^{-1})	$5.7\times10^{14}\exp\left(-\frac{36693.6}{RT}\right)$	15
k_{t3} (L mol^{-1} s^{-1})	0.001 (at 120°C), 0.01 (at 130°C)	16, 23

0.1°C). Further details about procedures and recovery of the polymer product from the ampoules have been documented earlier.[26]

Polymer characterization

Monomer conversion was measured gravimetrically. Number–average molecular weight and polydispersity were obtained by SEC or gel permeation chromatography (GPC). Two different setups were used in two different laboratories for independent replication and cross-checking of experimental results.

''GPC 1'' was a SEC/GPC setup with Viscotek's quad detector, comprised of a UV detector, low- (7°) and right-angle (90°) laser light-scattering detectors (LALLS/RALLS), differential refractometer, and viscometer in series. The laser wavelength was 670 nm. The *dn/dc* (specific refractive increment) value for PS was 0.185 mL/g. Analysis of data was performed with the OmniSEC v3.0 (Viscotek) software. The setup was equipped with one PLgel 10-μm guard column (50 × 7.5 mm) and three PLgel 10-μm MIXED-B columns (300 × 7.5 mm) (Polymer Laboratories). All columns and detectors were maintained at 30°C.

''GPC 2'' was a Waters Alliance 2695 equipment with Waters 2414 refractive index-, Viscotek viscometer- (model 270), and Waters 2996 UV detectors. Four columns (Shodex KF802, KF803, KF804 and KF806) in series were used in the set up. THF was filtered and used as the eluent at a flow rate of 1 mL/min. For both setups, polymer solutions of ~0.2 wt % were prepared and left for 12–24 h to fully dissolve the polymer and injection volumes between 100 and 200 μL were used.

MODELING

The polymerization mechanism used in this work is the same as the one proposed by Bonilla et al.[16] However, we did not use their model as in some of our previous contributions on NMRP.[21,23,24] Instead, we modeled the polymerization system using the Predici commercial software. We have demonstrated previously that the Bonilla et al.[16] model and the implementation of the same reaction mechanism in Predici (moments simulation mode) provide exactly the same results.[21,24] All the kinetic rate constants used in the calculations presented in this study are listed in Table II. With the exception of the free-volume parameters, which were used as adjusted parameters in some situations (as discussed below), all the remaining kinetic rate constants were fixed and taken from the literature.

Diffusion-controlled effects on the propagation, bimolecular radical termination, dormant polymer activation, and polymer radical deactivation reactions were modeled using free-volume theory.[21,27] The expressions used for the conversion-dependent kinetic rate constants of these reactions are summarized in Table III. v_f in the equations of Table III is the fractional free volume, whereas v_{f0} is the fractional free volume at initial conditions. The free volume parameters, β_t, β_p, β_a, and β_d are overlap factors for the termination, propagation, activation, and deactivation reactions, respectively. These overlap factors account for the fact that the same free volume is available to several molecules. They also account for molecule separation, once the molecules are in close proximity, but have not yet reacted.[27] T and T_{gi} are reaction temperature and glass transition temperature of component i, respectively, and α_i is the expansion coefficient for species i. V_i and V_t are volume of species i and total system volume, respectively.

The presence of prepolymer was first modeled as a solvent of high molecular weight, with free-volume parameters (α_i and T_{gi}) corresponding to PS. This is a good approximation for the case of inert prepoly-

TABLE III
Mathematical Expressions for Diffusion-Controlled Effects

Reaction or variable	Mathematical expression
Monomer propagation	$k_p = k_p^0 \exp\left[-\beta p\left(\frac{1}{v_f} - \frac{1}{v_{f0}}\right)\right]$
Bimolecular termination	$k_{tjn} = k_{tj}^0 \exp\left[-\beta_t\left(\frac{1}{v_f} - \frac{1}{v_{f0}}\right)\right], \quad j = c, d$ c, combination; d, disproportionation
Dormant polymer activation	$k_a = k_a^0 \exp\left[-\beta_a\left(\frac{1}{v_f} - \frac{1}{v_{f0}}\right)\right]$
Living polymer deactivation	$k_{da} = k_{da}^0 \exp\left[-\beta_d\left(\frac{1}{v_f} - \frac{1}{v_{f0}}\right)\right]$
Fractional free-volume	$v_f = \sum_{i=1}^{\text{No. of components}} \left[0.025 + \alpha_i\left(T - T_{gi}\right)\right] \frac{V_i}{V_t}$

mer, although it is inexact for the case of TEMPO-capped prepolymer (PS-TEMPO, represented by PPS I and PPS II in Table I), because the prepolymer in this last case can be activated and deactivated reversibly, thus participating in the reaction mechanism. Therefore, the cases with PS-TEMPO prepolymer (runs 1 and 2) were also modeled as a combination of bimolecular NMRP (TEMPO and BPO) and monomolecular NMRP (PS-TEMPO). In the second approach, the presence of the monomolecular controller (the PS-TEMPO controller) was considered in the calculations of free volume, with its α_i and T_{gi} values being the same as those of PS. Calculations of the concentration of PS-TEMPO controller accounted for the presence of dead polymer by running simulations of the NMRP production of the prepolymer at the conditions in which they were produced,[24] and estimating the content of dormant and dead polymer from those calculations. The effective concentrations of prepolymer used in the calculations are reported in brackets, in the last column of Table I.

The implementation of the Bonilla et al.[16] model in Predici is shown in Table IV. The presence of prepolymer as inert solvent of high molecular weight affects the concentrations of the species in the polymerization mixture (dilution effect) and the calculation of free volume. In the case of prepolymer behaving as monomolecular controller, the prepolymer was considered as added nitroxyl ether (NOe in Table IV), thus also affecting the calculation of free volume.

RESULTS AND DISCUSSION

Table I shows the experimental runs carried out in this study. Six different types of polystyrene prepolymer (referred to as PPS) were used in the study. They

TABLE IV
Model Implementation in Predici®

Reaction	Step	Name of step	Kinetic rate constant
Chemical initiation	$I \rightarrow 2I^*$ $I^* + M \rightarrow P^*$ (1)	Initiation(rad)	k_{di}, f
Nitroxyl ether decomposition	NOe $\leftrightarrow$ $NO_x^* + R^*$	Reversible reaction	k_{a2}, k_{d2}
Mayo dimerization	$M + M \rightarrow D$	Elemental reaction	k_{dim}
Thermal initiation	$D + M \rightarrow M^* + D^*$	Elemental reaction	k_{ia}
First propagation	$M^* + M \rightarrow P^*$ (1)	Initiation(anion)	k_p
First propagation	$R^* + M \rightarrow P^*$ (1)	Initiation(anion)	k_p
First propagation	$D^* + M \rightarrow P^*$ (1)	Initiation(anion)	k_p
Propagation	$P^*(s) + M \rightarrow P^*(s + 1)$	Propagation	k_p
Dormant-living exchange (monomeric alcoxyamine)	$NO_x^* + M^* \leftrightarrow MON_x$	Reversible reaction	k_d, k_a
Dormant-living exchange (polymeric alcoxyamine)	$P^*(s) + NO_x^* \rightarrow Pd(s)$	Change	k_d
Dormant-living exchange (polymeric alcoxyamine)	$Pd(s) \rightarrow P^*(s) + NO_x^*$	Change	k_a
Alcoxyamine decomposition	$MON_x \rightarrow M + HON_x$	Elemental reaction	k_{decomp}
Rate enhancement reaction	$D + NO_x^* \rightarrow D^* + HON_x$	Elemental reaction	k_{h3}
Termination	$P^*(s) + P^*(r) \rightarrow Pm(s + r)$, $P^*(s) + P^*(r) \rightarrow Pm(s) + Pm(r)$	Combination	k_{tc}, k_{td}
Chain transfer to monomer	$P^*(s) + M \rightarrow Pm(s) + M^*$	Change	k_{fm}
Chain transfer to dimer	$P^*(s) + D \rightarrow Pm(s) + D^*$	Change	k_{fd}

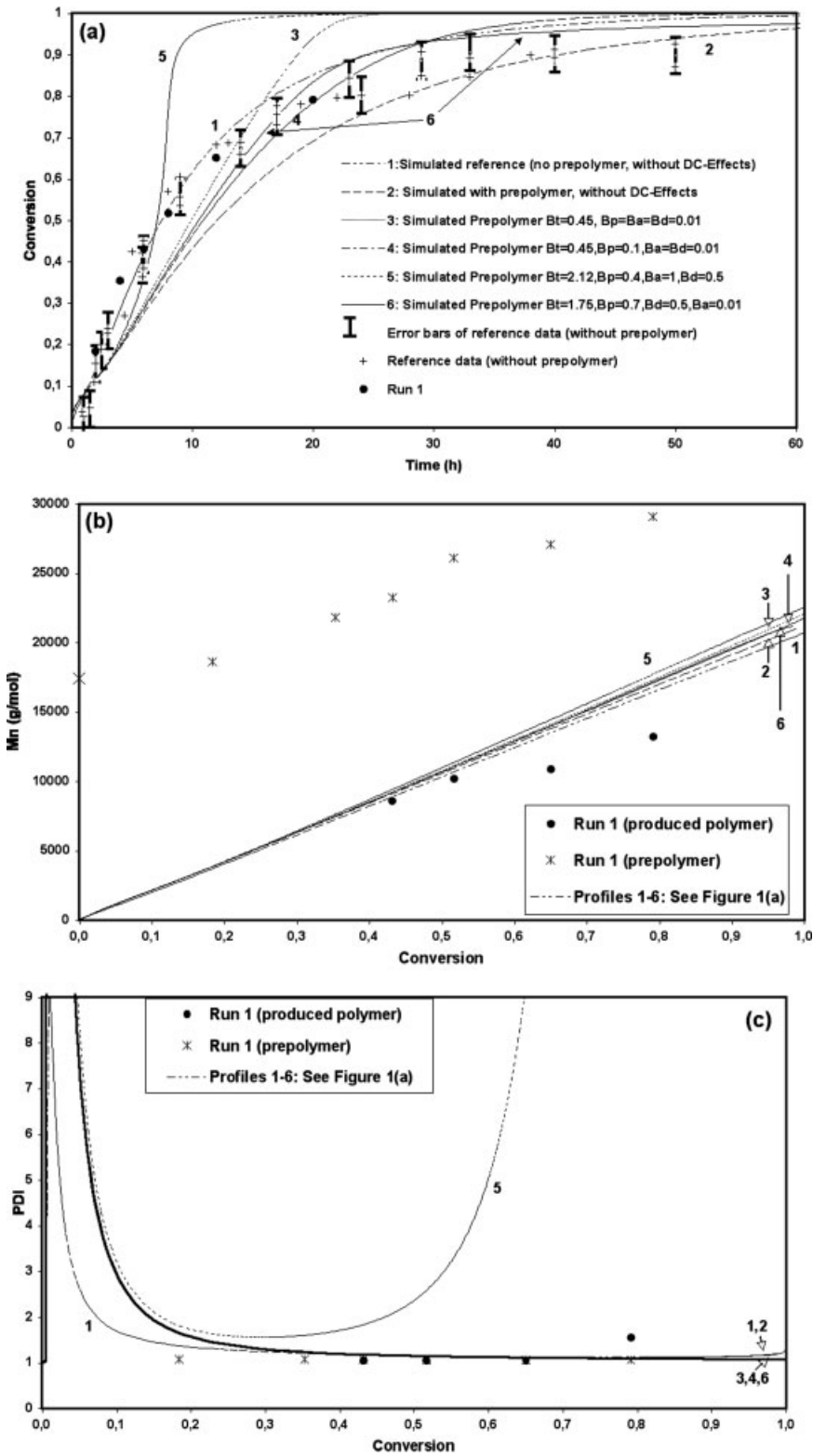

Figure 1 Comparison of experimental data and model predictions of (a) conversion versus time, (b) M_n versus conversion, and (c) PDI versus conversion, for run 1.

are identified as PPS I to PPS VI, with the identifier number increasing with the molecular weight of prepolymer. PPS I and PPS II were TEMPO-capped polymer molecules (PS-TEMPO), whereas PPS III to PPS VI consisted of inert PS synthesized by anionic polymerization (commercial PS standards for SEC).

From the experimental data gathered in this study, the experimental standard deviations for monomer

conversion, number–average molecular weight, and PDI, σ_x, σ_{M_n}, and σ_{PDI}, respectively, were determined. The calculated values were $\sigma_x = 0.022535$, $\sigma_{M_n} = 1700$ g mol^{-1}, and $\sigma_{PDI} = 0.05$. These standard deviations were used to calculate the magnitudes of the error bars shown in Figures 1 and 7.

The system with 44.94 wt % of nitroxyl-capped prepolymer (PS-TEMPO), $M_n = 17{,}400$ g mol^{-1} and PDI lower than 1.2 (PPS II), was used as the starting point in our analysis (run 1 of Table I). Given the high concentration of prepolymer, it was expected that DC effects would manifest more clearly and early in the reaction profile. Using the kinetic rate constants reported in Table II at the conditions (temperature) of run 1 and typical values for the free volume parameters, a simulation using Predici was carried out [profile 3 in Fig. 1(a)]. As observed, the predicted polymerization rate, expressed as conversion versus time, was significantly slower than the one obtained experimentally at low and intermediate conversions and much faster at high conversions [see Fig. 1(a)]. Different values of the free-volume parameters were tried (profiles 4–6), using as a guide the results obtained by Roa-Luna et al.,[21] until a better profile (number 6 in Fig. 1) was obtained. The estimation procedure thus consisted of determining the importance of the parameters by carrying out parameter sensitivity analyses, establishing bounds for the parameters from what is known about free-volume theory as applied to polymerization systems and carrying out single search parameter variation simulation runs.

Also shown in Figure 1(a) are experimental data[24] at the same polymerization conditions of this study, but without the presence of prepolymer in the recipe. In addition, simulated profiles for the case without prepolymer and neglecting DC effects (profile 1), as well as with prepolymer, but neglecting DC effects (profile 2) are also shown. It is interesting to note that the experimental data of conversion versus time using PPS II show a slightly faster polymerization rate than the case without prepolymer at low to intermediate conversions, but fall well within the experimental error at intermediate to high conversions (see error bars). Depending on the values of the free volume parameters used in the simulations, very different profiles of conversion versus time can be produced, although in some cases (profiles 5 and 6) the free-volume parameters used deviate significantly from the values observed in the literature for standard styrene polymerization (see, e.g., Vivaldo-Lima et al.[27]). However, in the case of ATRP of styrene, free-volume parameters similar to those used for profiles 5 and 6 of Figure 1(a) have been reported.[28] The case with the strongest autoacceleration effect (profile 5 in Fig. 1) also produces the highest deviation from living behavior, in terms of PDI versus conversion [profile 5 in Fig. 1(c)]. However, the presence of DC effects does not significantly affect the profiles of M_n versus conversion [Fig. 1(b)]. As in conventional radical polymerization, it is the weight–average molecular weight (M_w) and not the number–average molecular weight (M_n), which is more sensitive to the presence of DC effects.

Figure 2(a) shows the experimental data of conversion versus time for run 1, the predicted profile 6 (solid line) of Figure 1(a), and one new simulated profile obtained with the approach that the prepolymer (PS-TEMPO) behaves as a monomolecular NMRP controller. The new profile [dotted line in Fig. 2(a)], which assumes the added polymer acts as a NMRP controller, with the exact same parameters as profile 6 of Figure 1(a), shows exactly the same behavior up to about 50% monomer conversion, subsequently predicting a slightly slower polymerization rate, and finally (slightly) exceeding the original profile at about 35 h of polymerization. The small differences between the model traces are less than the observed range of scatter in experimental data points (e.g., in conversion versus time [Fig. 1(a)]). Therefore, there is little meaningful difference between the traces. From a practical point of view, the approach of considering the PS-TEMPO prepolymer as inert seems to be good enough for our modeling purposes, at the conditions studied in this work.

The profiles of M_n versus conversion for run 1, with a value of β_t of 1.75, corresponding to the simulations obtained with both models [prepolymer as inert solvent or as monomolecular controller, as in Figure 2(a) for monomer conversion], are shown in Figure 2(b). The corresponding profiles of PDI versus conversion are shown in Figure 2(c). It is observed that, in both cases [M_n and PDI versus conversion, Fig. 2(b,c), respectively], the predictions obtained with both models completely overlap, and the agreement between the predicted profiles and the experimental data shown in both figures is reasonably good.

Figure 3 shows predicted profiles of initiator, nitroxyl stable-free radical, and alcoxyamine monomolecular controller (PS-TEMPO prepolymer) concentrations versus time. As expected, it is observed that the initiator is consumed in less than 0.05 h (3 min). The concentration of nitroxyl stable-free radicals decreases sharply while the initiator is being consumed. The concentration of PS-TEMPO remains almost constant, which can be explained by the fact that it is part of an equilibrium reaction between dormant and living polymer that favors the dormant polymer.

Using the ''best'' parameters so far (among those analyzed previously, but not necessarily rigorously optimal) obtained for run 1 (with PPS II), the case with prepolymer of 900,000 g mol^{-1} (run 3, PPS V) was simulated with Predici (profile c in Fig. 4). The

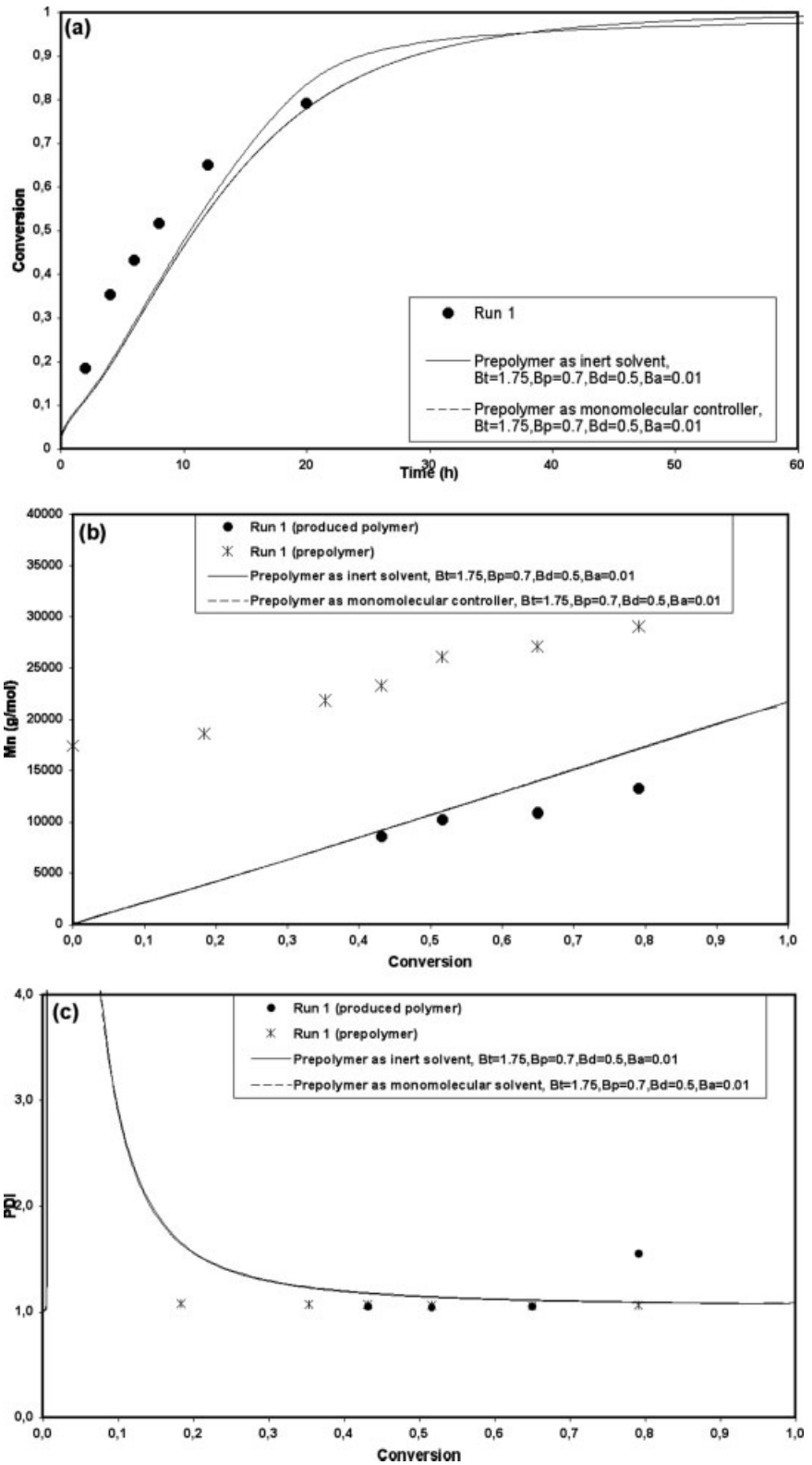

Figure 2 Comparison of experimental data and model predictions of (a) conversion versus time, (b) M_n versus conversion, and (c) PDI versus conversion, for run 1, using an improved model (prepolymer as monomolecular controller).

simulations in Figure 4 were produced with the approach that the added prepolymer behaves as an inert ''solvent'' of high molecular weight, which is correct in this case. The predicted polymerization rate [profile c in Fig. 4(a)] was faster than the one obtained experimentally. The free volume parameters for DC-termination and DC-deactivation were fine tuned, until a better agreement for poly-

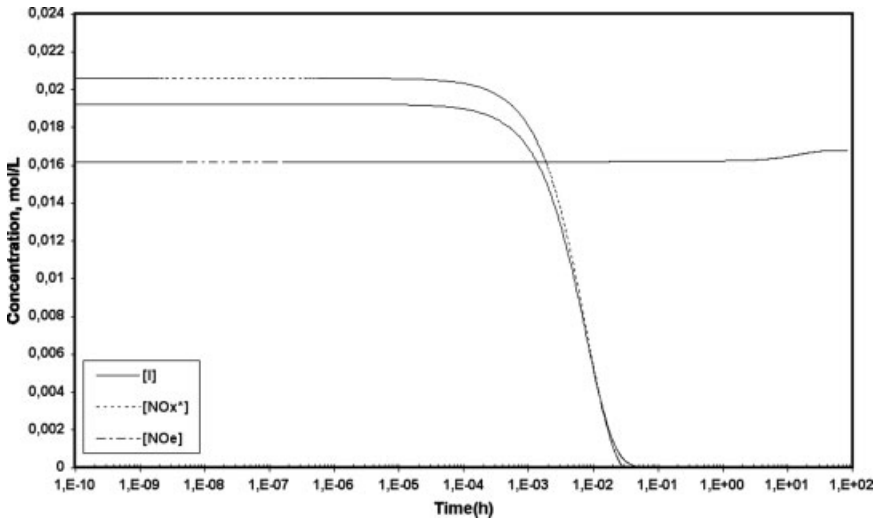

Figure 3 Calculated profiles of concentrations of initiator, nitroxyl stable free radicals, and alcoxyamine, for run 1, obtained with the improved model (prepolymer as monomolecular controller).

merization rate [profile a in Fig. 4(a)] was obtained, although the predictions for M_n [see Fig. 4(b)] did not improve. Also shown in Figure 4(a), for comparison purposes, are the experimental data corresponding to runs 1 and 2. Although there seems to be some distinction between the three runs, the differences are not fully clear. The fact that the polymerization rate for run 2 is faster than run 1 can be explained by the fact that the TEMPO/BPO ratio is lower in run 2. The fact that the polymerization rate is the lowest for run 3 may be explained by the fact that the TEMPO/BPO ratio is slightly higher in this run. The case of inert prepolymer will be further analyzed below in the analysis of runs 4–6.

It is observed in Figure 4(b) that the simulated profile of M_n versus conversion underpredicts the data, irrespective of the free volume parameters used, a situation also observed for the case without prepolymer, using the parameters of Table II.[21,24] In the case of PDI versus conversion [Fig. 4(c)], the model predicts high PDIs at low conversions, a situation also observed in the case without prepolymer.[21,23,24] However, in this case, the range of large PDIs extends to higher conversions, and it is only around 60% monomer conversion that the simulated profiles agree to a reasonable degree with the experimental data.

Using the best parameters of the previous case (PPS V, run 3), the polymerization conditions of the system with prepolymer of 6,084 g mol^{-1} (PPS I, run 2) were simulated. Figure 5 shows experimental data and calculated profiles of conversion versus time [Fig. 5(a)], M_n versus conversion [Fig. 5(b)], and PDI versus conversion [Fig. 5(c)], for run 2. The profiles shown in Figure 5 were produced taking into account the reactive nature of the PS-TEMPO prepolymer, that is, when the prepolymer is modeled as a monomolecular controller. One simulation carried out with the inert ''solvent'' approach (solid line) was also included in Figure 5. The agreement between experimental data and model predictions is better when $\beta_t = 1.75$, as in run 1. The differences obtained between the two modeling approaches are negligible in this case, which may be explained by the very low molar concentration of prepolymer used in run 3. The calculated profiles of concentration versus time for initiator, nitroxyl stable-free radicals, and alcoxyamine controller shown in Figure 6 exhibit the same qualitative features as those described earlier for run 1 (Fig. 3).

Thus far, it has been observed that, as expected, a better fit to experimental data can be obtained if the free-volume parameters are fine tuned. However, the changes obtained in the profiles produced are not that significant, considering that even the case without DC effects provides a reasonable fit.

Figure 7(a) shows the experimental data and predicted profiles of conversion versus time for runs 4–6. The same free-volume parameters as in runs 2 and 3 were used for runs 4–6. It is observed that runs 4–6 practically overlap, an effect well captured by the simulations, because the simulated profiles 4–6 also overlap. Overall, the effect of the molecular weight of inert prepolymer was well captured by the model behind the simulations carried out using Predici, although the qualitative agreement was not as good at high conversions. This mismatch may be explained by the inaccuracies in the kinetic rate constants and has been discussed in depth in Roa-Luna et al.[24]

Similar observations as those mentioned earlier for polymerization rate can be made for the evolution of number–average molecular weight [Fig. 7(b)] and PDI [Fig. 7(c)] versus conversion. It is observed in

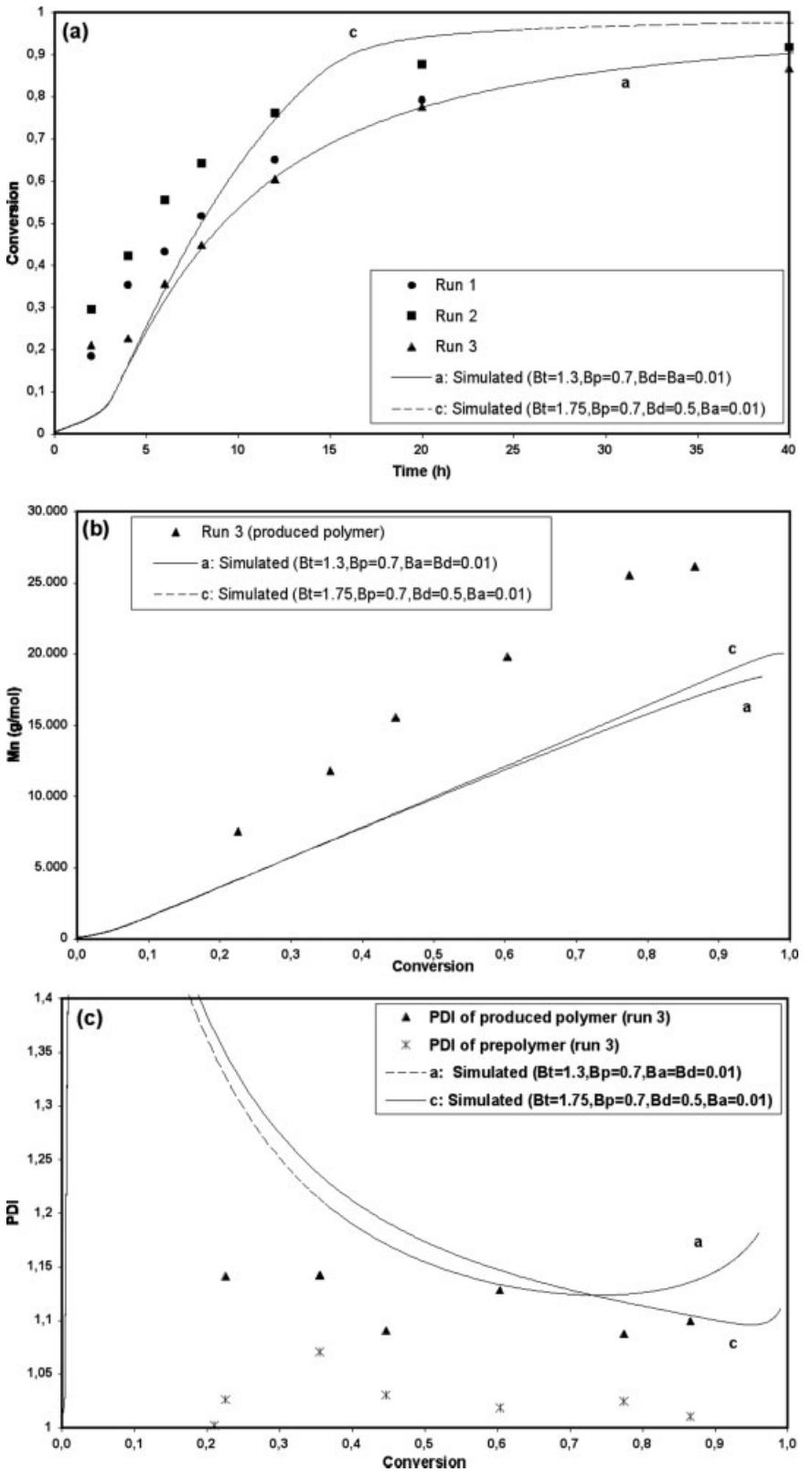

Figure 4 Comparison of experimental data and model predictions of (a) conversion versus time, (b) M_n versus conversion, and (c) PDI versus conversion, for run 3.

Figure 7(b,c) that the values of M_n measured with GPC 2 are systematically higher, and the values of PDI systematically lower, than those measured using GPC 1. Although GPC 2 had three detectors, the measurements of M_n and PDI shown in Figure 7 were obtained with only one detector (the refractive

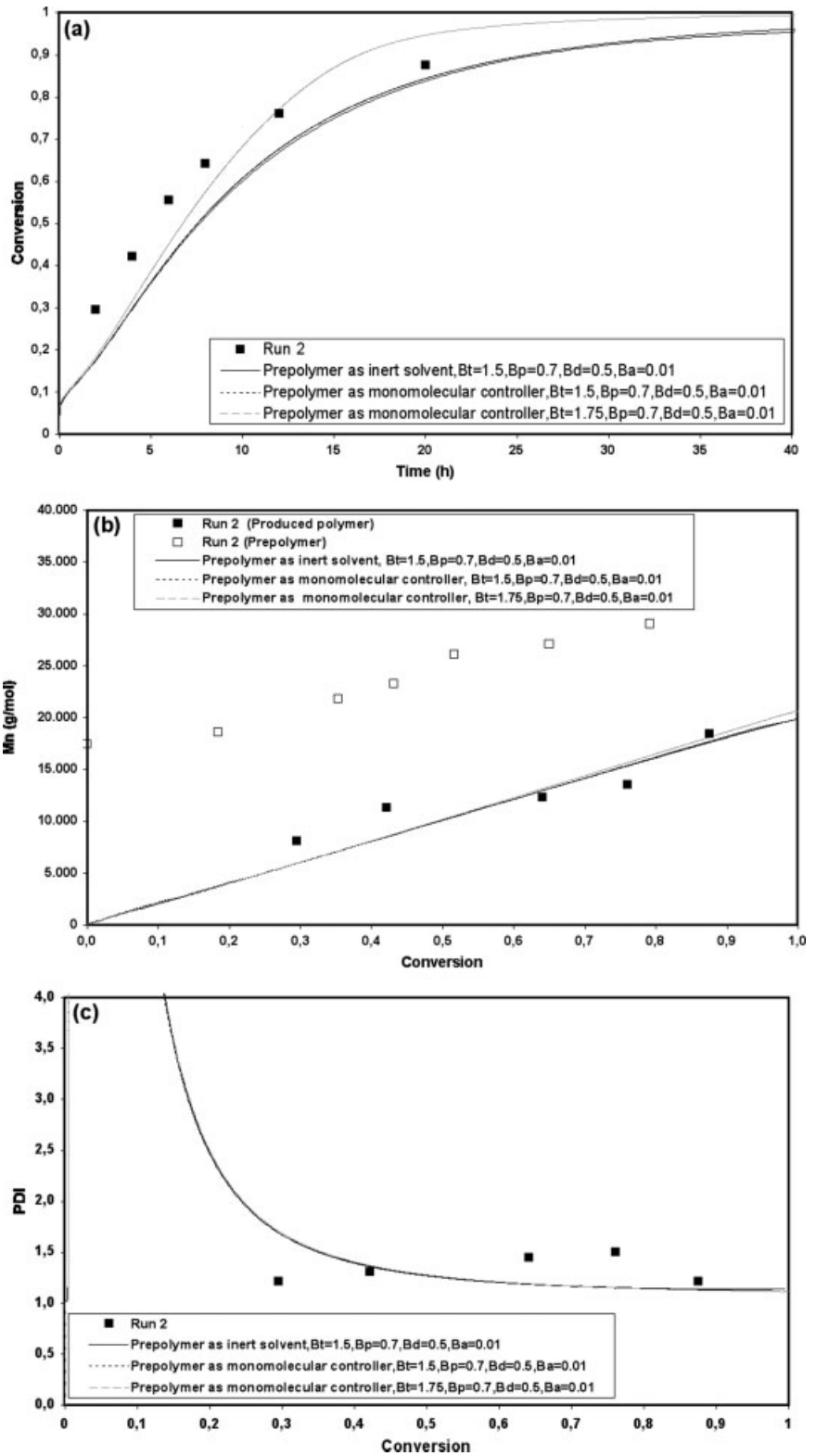

Figure 5 Comparison of experimental data and model predictions of (a) conversion versus time, (b) M_n versus conversion, and (c) PDI versus conversion, for run 2, comparing the two models of this work.

index). It is also observed that the experimental error is rather large, and the two sets lie within the error bars. Because many researchers in the area of CRP report molecular weight measurements with single detector systems, we decided to include these measurements, as a way to stress the importance of taking into consideration or at least be aware of some of the different possible sources of experimental

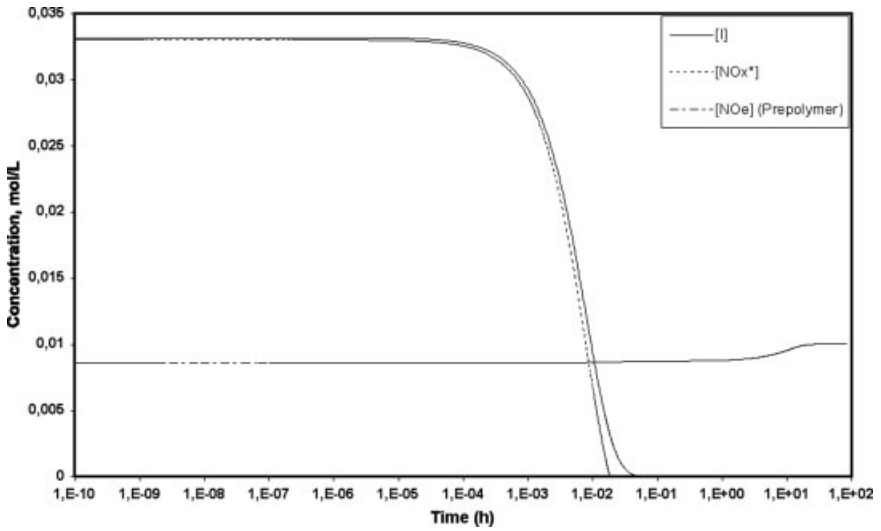

Figure 6 Calculated profiles of concentrations of initiator, nitroxyl stable free radicals, and alcoxyamine, for run 2, obtained with the improved model (prepolymer as monomolecular controller).

uncertainty in polymerization studies. A more in-depth discussion of these issues can be found in Roa-Luna et al.[24] The quantitative discrepancies between experimental and predicted profiles may once again be explained in terms of potentially inaccurate kinetic rate constants used in the simulations, as explained by Roa-Luna et al.[24] However, another plausible explanation for that deviation may be a loss of TEMPO because of participation in ''promoted dissociation'' of BPO, proposed by Moad et al.[29] and further clarified by Georges et al.[30]

Georges et al.[30] suggested that as much as 50% of TEMPO may be lost in a reaction system consisting of TEMPO, BPO, and styrene at 70°C. That loss of TEMPO was reported to be less important at higher temperatures. To take into account the ''promoted dissociation'' effect in our model, we carried out additional simulations at the conditions of run 4, but lowering the concentration of TEMPO by 20 and 30%. As observed in Figure 7(a), a reduction of 30% in the TEMPO concentration (attributed to the ''promoted dissociation'' of BPO reaction) produced a noticeable acceleration in polymerization rate during the first minutes of reaction, but the overall profile did not change significantly. This initial acceleration was less pronounced in the case with a 20% TEMPO reduction [profile not shown in Fig. 7(a) to make visualization of the effect easier]. Running the simulations with a reduced effective concentration of TEMPO significantly improved the agreement between model predictions and experimental data of M_n versus conversion [see the profiles indicated as 20 and 30% in Fig. 7(b)]. The best agreement was obtained when a loss in TEMPO of 30% was assumed. However, assuming losses of 20 and 30% in TEMPO produced higher calculated PDIs at low conversions [see Fig. 7(c)]. Therefore, the effective concentration of TEMPO in our system may have been reduced by 30%. This reduction in TEMPO concentration may be large if one considers the high polymerization temperature used in our experiments (Georges et al.[30] concluded that the promoted dissociation of BPO is important at temperatures lower than 80°C). However, during the preparation and handling of the ampoules, the reaction stock solutions are maintained at ambient temperatures for significant periods and that may explain a significant loss in TEMPO concentration.

These results indicate that the disagreement between model predictions and experimental data of conversion versus time (at high conversions) and M_n versus conversion may be caused by a combination of having imprecise parameter estimates and because of the ''promoted dissociation'' of BPO, and other possible side reactions that may take place in the early stages of the polymerization. The net effect of these side reactions is to decrease the effective concentration of the controller.

Our modeling approach for the ''promoted dissociation'' of BPO considered that a fixed amount of TEMPO was lost at the beginning of the polymerization. The fact that our model simulations for 20–30% reduction of TEMPO fitted well the higher conversion range of PDI versus conversion [see Fig. 7(c)], whereas the lower/intermediate region was better represented with the profile without TEMPO reduction, may suggest that a gradual reduction of TEMPO along the reaction time is taking place. This gradual reduction of TEMPO was not used in our model but could be considered in future modeling studies.

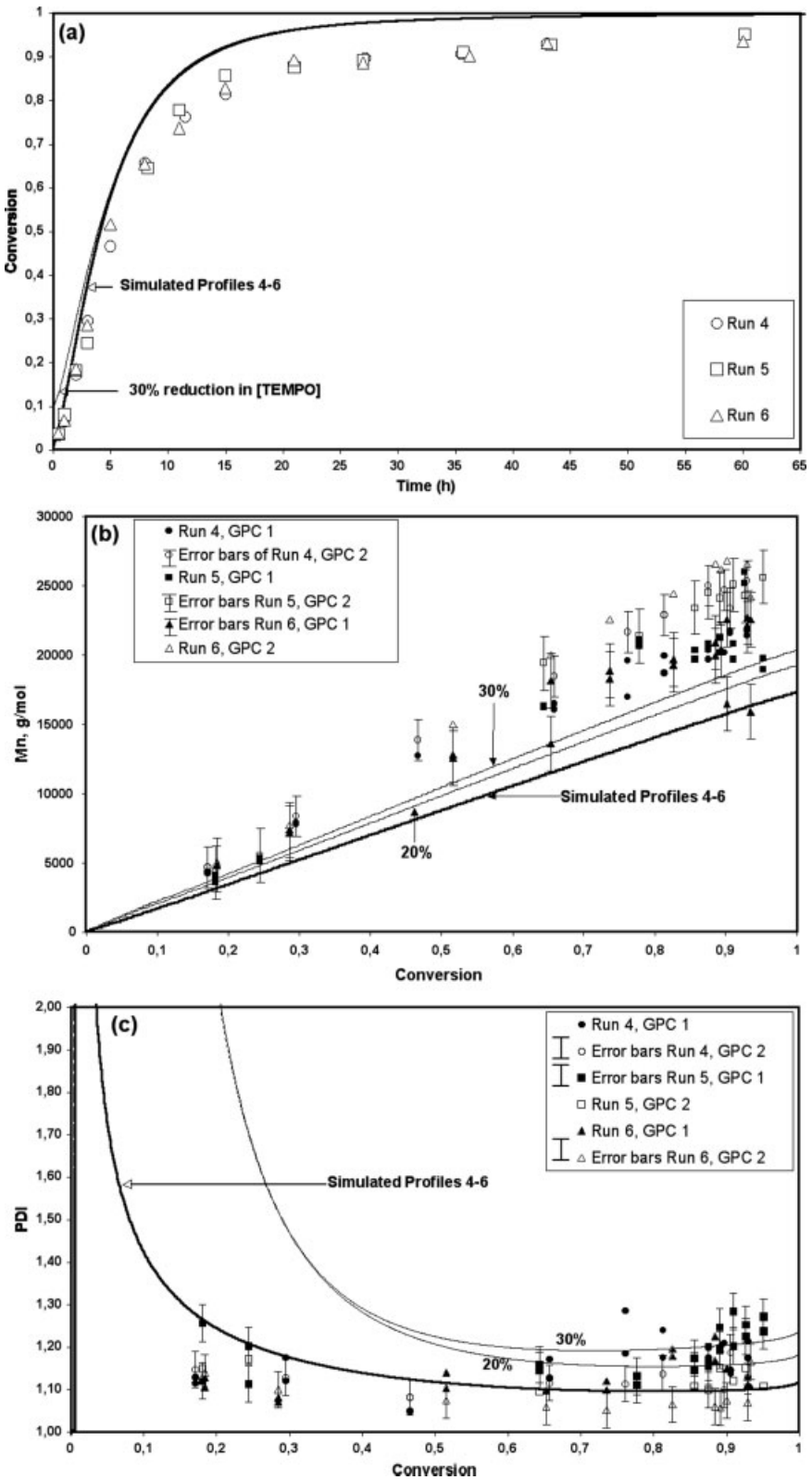

Figure 7 Comparison of experimental data and model predictions of (a) conversion versus time, (b) M_n versus conversion, and (c) PDI versus conversion, for runs 4–6.

CONCLUSIONS

Several experimental runs with prepolymer present and corresponding modeling efforts have shown that the agreement between experimental data and model predictions is slightly improved when the reactive character of the prepolymer (in the cases where PS-TEMPO is used as prepolymer) is incorporated into the model, using the approach that the added prepolymer behaves as an extra monomolecular NMRP controller. The disagreement observed in our analysis (mainly in M_n) can be explained in terms of the potential inaccuracy of some of the kinetic rate constants,[24] or possible side reactions which decrease the effective concentration of TEMPO, such as the ''promoted dissociation'' of BPO.[30]

Overall, based on our investigations so far, DC effects seem to be insignificant. The low importance of DC effects in NMRP is related to the moderately short molecules (when compared with the chain lengths typical of conventional radical polymerization) present in CRP processes as well as to the typical operating temperatures being well above the T_g of the resulting polymer.

NOMENCLATURE

D	Dimer
$D^\bullet$	Dimeric free radical
f	Initiator efficiency
HON_x	Hydroxylamine
I	Initiator
$I^\bullet$	Primary free radical from initiator
k_a	Dormant polymer activation kinetic rate constant (s^{-1})
k_{a2}	Activation rate constant in the nitroxyl ether decomposition reaction (s^{-1})
k_d	Kinetic rate constant for initiation decomposition (s^{-1})
k_{d2}	Deactivation rate constant in the nitroxyl ether decomposition reaction (s^{-1})
k_{da}	Polymer radical deactivation kinetic rate constant (L mol^{-1} s^{-1})
k_{decomp}	Kinetic rate constant for the alcoxyamine decomposition reaction (s^{-1})
k_{dim}	Kinetic rate constant for the dimerization reaction (L mol^{-1} s^{-1})
k_{fd}	Transfer to dimer kinetic rate constant (L mol^{-1} s^{-1})
k_{fm}	Transfer to monomer kinetic rate constant (L mol^{-1} s^{-1})
k_{h3}	Kinetic rate constant for the rate enhancement reaction (L mol^{-1} s^{-1})
k_{ia}	Kinetic rate constant for first propagation reaction (L mol^{-1} s^{-1})
k_p	Propagation kinetic rate constant (L mol^{-1} s^{-1})
k_{tc}	Termination by combination kinetic rate constant (L mol^{-1} s^{-1})
k_{td}	Termination by disproportionation kinetic rate constant (L mol^{-1} s^{-1})
k_{tjn}	Number-average termination kinetic rate constant, L mol^{-1} s^{-1} (subscript j accounts for either combination or disproportionation)
k_{th}	Kinetic rate constant for thermal initiation (L mol^{-1} s^{-1})
M	Monomer
$M^\bullet$	Monomeric free radical
MNO_x	Monomeric alcoxyamine
NO_e	Nitroxyl ether (or alcoxyamine) controller
$NO_x^\bullet$	Nitroxyl stable-free radical
$P^\bullet(s)$	Polymeric free radical of size s
$Pd(s)$	Dormant polymer of size s
$Pm(s)$	Dead polymer of size s
$R^\bullet$	Primary free radical obtained from the nitroxyl ether decomposition reaction
T	Temperature (K or °C)
T_g	Glass transition temperature (K or °C)
v_f	Fractional free volume
V_i	Volume of species i (L)
V_t	System volume (L)

Greek letters

α_i	Volumetric expansion coefficient of component i (K^{-1})
β_a	Free volume parameter for the activation reaction
β_d	Free volume parameter for the deactivation reaction
β_p	Free volume parameter for the propagation reaction
β_t	Free volume parameter for the termination reaction
σ_x	Experimental standard error of conversion
σ_{M_n}	Number–average molecular weight (g mol^{-1})
σ_{PDI}	Standard error of polydispersity

We acknowledge fruitful discussions with Drs. Ramiro Guerrero-Santos (CIQA, México) and Larissa Alexandrova (IIM-UNAM, México), who independently suggested adding a prepolymer to the initial mixture to capture DC effects from early on in the reaction, as well as with Dr. Enrique Saldívar-Guerra (CIQA) in the early stages of the project.

References

1. Matyjaszewski, K. In Advances in Controlled/Living Radical Polymerization; Matyjaszewski, K., Ed.; American Chemical Society: Washington, DC, 2003; A. C. S. Symposium Series 854, Chapter 1, pp 2–9.
2. Pirrung, F. O. H.; Quednau, P. H.; Auschra, C. Chimia 2002, 56, 170.

3. Auschra, C.; Eckstein, E.; Mühlebach, A.; Zink, M. O.; Rime, F. Prog Org Coat 2002, 45, 83.
4. Pirrung, F. O. H.; Auschra, C. Polym Prepr 2005, 46, 316.
5. Hawker, C. J. In Handbook of Radical Polymerization; Matyjaszewski, K.; Davis, T. P., Eds.; Wiley: Hoboken, 2002; Chapter 10, pp 463–522.
6. Fukuda, T.; Goto, A.; Tsujii, Y. In Handbook of Radical Polymerization; Matyjaszewski, K., Davis, T. P., Eds.; Wiley: Hoboken, 2002; Chapter 9, pp 407–462.
7. Goto, A.; Fukuda, T. Prog Polym Sci 2004, 29, 329.
8. Yoshikawa, C.; Goto, A.; Fukuda, T. Macromolecules 2002, 35, 5801.
9. Fischer, H. Chem Rev 2001, 101, 3581.
10. Le Mercier, C.; Acerbis, S. B.; Bertin, D.; Chauvin, F.; Gigmes, D.; Guerret, O.; Lansalot, M.; Marque, S.; Le Moigne, F.; Fischer, H.; Tordo, P. Macromol Symp 2002, 182, 225.
11. Souaille, M.; Fischer, H. Macromolecules 2001, 34, 2830.
12. Souaille, M.; Fischer, H. Macromolecules 2002, 35, 248.
13. Fischer, H. In Advances in Controlled/Living Radical Polymerization; Matyjaszewski, K., Ed.; American Chemical Society: Washington, DC, 2003; A. C. S. Symposium Series 854, Chapter 3.
14. Saldívar-Guerra, E.; Bonilla, J.; Becerril, F.; Zacahua, G.; Albores-Velasco, M.; Alexander-Katz, R.; Flores-Santos, L.; Alexandrova, L. Macromol Theory Simul 2006, 15, 163.
15. Zhang, M.; Ray, W. H. J Appl Polym Sci 2002, 86, 1630.
16. Bonilla, J.; Saldívar, E.; Flores-Tlacuahuac, A.; Vivaldo-Lima, E.; Pfaendner, R.; Tiscareño-Lechuga, F. Polym React Eng 2002, 10, 227.
17. Kruse, T. M.; Souleimonova, R.; Cho, A.; Gray, M. K.; Torkelson, J. M.; Broadbelt, L. Macromolecules 2003, 36, 7812.
18. Butté, A.; Storti, G.; Morbidelli, M. Chem Eng Sci 1999, 54, 3225.
19. Faliks, A.; Yetter, R. A.; Floudas, C. A.; Wei, Y.; Rabitz, H. Polymer 2001, 42, 2061.
20. Díaz-Camacho, F.; López-Morales, S.; Vivaldo-Lima, E.; Saldívar-Guerra, E.; Vera-Graziano, R.; Alexandrova, L. Polym Bull 2004, 52, 339.
21. Roa-Luna, M.; Díaz-Barber, M. P.; Vivaldo-Lima, E.; Lona, L. M. F.; McManus, N.; Penlidis, A. J Macromol Sci A: Pure Appl Chem 2007, 44, 193.
22. Chevalier, C.; Guerret, O.; Gnanou, Y. In Advances in Controlled/Living Radical Polymerization; Matyjaszewski, K., Ed.; American Chemical Society: Washington, DC, 2003; ACS Symposium Series 854, Chapter 30, pp 424–437.
23. Belicanta-Ximenes, J.; Mesa, P. V. R.; Lona, L. M. F.; Vivaldo-Lima, E.; McManus, N. T.; Penlidis, A. Macromol Theory Simul 2007, 16, 194.
24. Roa-Luna, M.; Nabifar, A.; Díaz-Barber, M. P.; McManus, N. T.; Vivaldo-Lima, E.; Lona, L. M. F.; Penlidis, A. J Macromol Sci A: Pure Appl Chem 2007, 44, 337.
25. Tuinman, E.; McManus, N. T.; Roa-Luna, M.; Vivaldo-Lima, E.; Lona, L. M. F.; Penlidis, A. J Macromol Sci A: Pure Appl Chem 2006, 43, 995.
26. McManus, N. T.; Penlidis, A. J Polym Sci Part A: Polym Chem 1996, 34, 237.
27. Vivaldo-Lima, E.; Hamielec, A. E.; Wood, P. E. Polym React Eng 1994, 2, 17.
28. Delgadillo-Velázquez, O.; Vivaldo-Lima, E.; Quintero-Ortega, I. A.; Zhu, S. AIChE J 2002, 48, 2597.
29. Moad, G.; Rizzardo, E.; Solomon, D. H. Tetrahedron Lett 1981, 22, 1165.
30. Georges, M. K.; Hamer, G.; Szkurhan, A. R.; Kazemedah, A.; Li, J. Polym Prepr 2002, 43, 78.